Astron. Astrophys. 362, 97–104 (2000)

ASTRONOMY AND ASTROPHYSICS

On the degree of dust extinction in major galaxy mergers with dusty starburst

K. Bekki[1] **and Y. Shioya**[2]

[1] Division of Theoretical Astrophysics, National Astronomical Observatory, Mitaka, Tokyo, 181-8588, Japan (bekki@th.nao.ac.jp)
[2] Astronomical Institute, Tohoku University, Sendai, 980-8578, Japan (shioya@astr.tohoku.ac.jp)

Received 28 April 2000 / Accepted 8 August 2000

Abstract. We numerically investigate how fundamental properties of the spectral energy distribution (SED) of a major gas-rich galaxy merger with dusty starburst are determined by the initial orbital configuration of the merger. We found that an infrared luminous galaxy with dusty starburst formed by a nearly retrograde-retrograde merger suffers the most remarkable dust extinction of stellar light and consequently shows very red colours. Considering that a retrograde-retrograde merger does not produce strong and long tidal tails, this result suggests that a luminous infrared galaxy without clear signs of interaction and merging shows very large internal dust extinction and redder colours. These numerical results furthermore imply that the morphology of a luminous infrared galaxy can correlate with the degree of internal dust extinction and thus with the shape of the SED, principally because the morphology of a merger also depends strongly on the initial orbital configuration of the merger. Based on these results, we discuss the origin of ultra-luminous infrared galaxies.

Key words: galaxies: interactions – galaxies: ISM – galaxies: kinematics and dynamics

1. Introduction

Ultra-luminous infrared galaxies (ULIRGs), which are ongoing major mergers between gas-rich spirals, are generally considered to provide valuable clues to the understanding not only for the formation processes of elliptical galaxies and active galactic nuclei (AGN) but also for the nature of high redshift dusty starburst galaxies (Sanders et al. 1988; Sanders & Mirabel 1996; Meurer et al. 1999; Trentham et al. 1999). In particular, to investigate how and to what degree stellar light is heavily obscured by dust in low redshift ULIRGs may lead us to clarify the origin even for high redshift faint sub-millimeter sources recently discovered by the Sub-millimeter Common-User Bolometer Array (SCUBA) (Holland et al. 1999) on the James Clerk Maxwell Telescope (Smail et al. 1997; Hughes et al. 1998; Smail et al. 1998; Barger et al. 1998; Lilly et al. 1999). Recently, Trentham et al. (1999) have found that the degree of internal dust extinction at optical and ultraviolet wavelength in the spectral energy distribution (SED) of ULIRGs is very different between ULIRGs, though the total number of the sample ULIRGs is very small (only 3). They furthermore showed that the magnitude of the drop of SEDs from optical to ultraviolet band ranges from a factor of ~ 3 in IRAS F22491-1808 to a factor of ~ 100 in VII Zw 031. The derived SEDs of ULIRGs from ultraviolet to near-infrared band not only help us to understand the physical relationship between low redshift ULIRGs and high redshift faint SCUBA sources (Trentham et al. 1999) but also provides valuable information on an evolutionary link between faint SCUBA sources with blue $V-I$ colour (~ 1.5 mag) observed by Smail et al. (1998) and Extremely Red Objects (EROs) first discovered by Elston et al. (1988). It is, however, not clear at all what controls the degree of internal dust extinction in ULIRGs.

The purpose of this paper is to investigate what determines the nature of SEDs and the degree of internal dust extinction in ULIRGs by performing numerical simulations that can follow chemodynamical and photometric evolution of major galaxy mergers with dusty interstellar gas in an explicitly self-consistent manner. We here consider the global dynamical evolution of galaxy mergers, which depends strongly on initial orbital configurations of mergers (i.e., whether a merger is prograde-prograde one or retrograde-retrograde one), is one of primarily important factors for the SEDs of ULIRGs. Mihos & Hernquist (1996) have already investigated in detail the $gas\ dynamical\ evolution$ of major mergers and demonstrated that internal structure of merger progenitor disks (i.e., whether a disk has a strong bulge or not) rather than orbital configurations is a key factor for the merger star formation history. However they did not discuss the nature of SEDs of ULIRGs. Therefore our present results are complementary to their important results in the sense that we can demonstrate how the $SEDs$ of mergers can depend on initial physical conditions of major mergers. A remarkable difference between the present study and previous ones that investigate SEDs of galaxies (e.g., Mazzei et al. 1992; Franceschini et al. 1994; Gordon et al. 1997; Guiderdoni et al. 1998) is that dynamical effects on stellar and gaseous distributions are included in the present study. We suggest that the SED of an ULIRG depends on the orbital configuration of a merger and furthermore that the SED of the ULIRG can correlate strongly with its morphology. Physical correlations between

Send offprint requests to: K. Bekki

morphological properties and SEDs in ULIRGs have not been discussed so extensively in previous studies. The present numerical results thus shed new light on formation and evolution of ULIRGs.

2. Model

We here investigate both temporal evolution of galactic morphology and that of SED, based on numerical simulations that can follow both dynamical and chemical evolution of galaxies. The numerical techniques for solving galactic chemodynamical and photometric evolution and the methods for deriving SEDs in numerical simulations of galaxy mergers with dusty starburst are given in Bekki & Shioya (1999) and Bekki et al. (1999), respectively. Accordingly we describe only briefly the present numerical model of dusty starburst galaxy mergers here. The physical parameters used in this paper are very similar to those adopted by Bekki et al. (1999) and plausible and realistic for gas-rich major mergers. We construct models of galaxy mergers between gas-rich disk galaxies with equal mass by using Fall-Efstathiou model (1980). The total mass and the size of a progenitor disk are 6.0×10^{10} $\mathrm{M}_{\odot}$ and 17.5 kpc, respectively. The collisional and dissipative nature of the interstellar medium with the initial gas mass fraction f_{g} = 0.2 is modeled by the sticky particle method (Schwarz 1981). Star formation is modeled by converting the collisional gas particles into collisionless new stellar particles according to the Schmidt law (Schmidt 1959) with the exponent of 2.0. As long as the exponent ranges from 1.5 to 2.0, our numerical results do not depend so strongly on the exponent of the Schmidt law. Chemical enrichment through star formation during galaxy merging is assumed to proceed both locally and instantaneously in the present study. The fraction of gas returned to interstellar medium in each stellar particle and the chemical yield are 0.3 and 0.02, respectively. Initial metallicity Z_{*} for each stellar and gaseous particle in a given galactic radius R (kpc) from the center of a disk is given according to the observed relation $Z_{*} = 0.06 \times 10^{-0.197 \times (R/3.5)}$ of typical late-type disk galaxies (e.g., Zaritsky et al. 1994).

In the present study, we consider that the most important parameter for determining morphological and photometric evolution of a galaxy merger is an initial orbital configuration of the merger. We accordingly investigate merger models with variously different orbital configurations. We here present the results of two models, a nearly prograde-prograde model (referred to as PP model for convenience), and a nearly retrograde-retrograde one (RR). The reason for this adoption is that these models clearly show the most remarkable differences in the morphological and photometric evolution of galaxy mergers between these two. The results for models with variously different orbital configurations will be described in detail by Bekki & Shioya (2000). The angle between intrinsic spin vector and orbital one in one disk for each of mergers is set to be 30 degrees. The orbital plane of a galaxy merger is assumed to be the same as x-y plane and the initial distance between the center of mass of merger progenitor disks is 140 kpc. Two disks in the merger are assumed to encounter each other parabolically with the pericentric distance of 17.5 kpc.

Structural and kinematical properties of merger remnants, star formation history of mergers with prominent bulges, and that of dusty starburst mergers between bulgeless spirals have been already given in Barnes & Hernquist (1992), Mihos & Hernquist (1996), and Bekki et al. (1999), respectively. Thus we describe only morphological and photometric properties of mergers between two gas-rich bulgeless disk galaxies $at\ the\ epoch\ of\ massive\ starburst$ in the present study. For calculating the SED of a merger, we use the spectral library GISSEL96 which is the latest version of Bruzual & Charlot (1993). Using the derived SED, we also investigate how dust-enshrouded starburst galaxy mergers at z=0.4 and 1.0 can be seen with the $Hubble\ Space\ Telescope$ (HST). The method to construct the synthesized HST images of galactic morphology in the present study is basically the same as that described by Mihos (1995). For calculating the SED of a merger at z=0.4 and 1.0, we assume that mean ages of old stellar components initially in a merger progenitor disk at the redshift z=0.4 and 1.0 are 7.14 and 3.80 Gyr, respectively. The V band apparent magnitude m_V, global colours ($B-V$, $V-R$, $V-I$, $R-K$, and $I-K$), and $S_{850\,\mu\mathrm{m}}$ flux at each redshift (z=0.4, 1, 1.5, 2, and 3) for the two models (PP and RR) are summarized in the Table 1. In the followings, the cosmological parameters H_0 and q_0 are set to be 50 km s^{-1} Mpc^{-1} and 0.5 respectively.

3. Results

Fig. 1 shows star formation history both for the PP and RR models. Although the strength of the maximum starburst is not very different between the two models, the epoch of the starburst is very different. The massive starburst is triggered in the first encounter for the PP model whereas the starburst occurs only in the late merger phase when the two cores merge to form a single (elliptical) galaxy for the RR model. Accordingly the separation of two galactic cores at the starburst epoch is very different (This is described in detail later in Fig. 3 and Fig. 4). The essential reason for this difference is that strong stellar bars, which can drive a large amount of interstellar gas into the central region and thus trigger massive starburst, can be formed in the first encounter $only$ for the PP model. This result that orbital configuration of major galaxy merging is an important determinant for merger star formation history is in striking contrast to the previous numerical results by Mihos & Hernquist (1996). They demonstrated that internal structure of merger progenitor disks (i.e., whether a disk has a remarkable bulge or not) rather than orbital configurations is a key factor for the merger star formation history. The reason for this apparent difference between the present results and those by Mihos & Hernquist (1996) is essentially that we do not include bulges at all in the present merger simulations. As pointed out by Mihos & Hernquist (1996), irrespectively of merger orbital configurations, massive starburst occurs in the late merger phase when two cores merge to form an elliptical galaxy for mergers with remarkable bulges (with the mass ratio of bulge to disk $\sim$ 0.3:1),

Table 1. The redshift evolution of V band magnitude, colours, and 850 μm flux for the PP model and the RR one. For z = 0 (actually = 0.017 similar to the redshift of Arp 220), upper and lower values represent the results of the model without dust extinction and those of the model with dust extinction, respectively. For the models without dust extinction at z = 0, the absolute magnitude is given whereas for z $\geq$ 0, the apparent one is given in each of the two models with dust extinction.

z	m_V	$B-V$	$V-R$	$V-I$	$R-K$	$I-K$	$S_{850\,\mu\mathrm{m}}$ (mJy)
				PP model			
z=0.0	-22.02	0.245	0.297	0.669	2.171	1.800	0
z=0.0	14.37	0.878	0.593	1.123	2.526	1.996	5.38×10^2
z=0.4	22.59	1.175	1.321	2.116	3.707	2.913	3.07
z=1.0	25.97	0.696	0.927	2.011	5.376	4.291	2.15
z=1.5	27.31	0.420	0.637	1.606	5.962	4.992	1.83
z=2.0	28.07	0.375	0.464	1.124	6.074	5.413	1.58
z=3.0	29.15	1.334	0.488	0.976	5.919	5.430	1.25
				RR model			
z=0.0	-21.94	0.280	0.320	0.698	2.209	1.832	0
z=0.0	14.61	0.953	0.628	1.185	2.674	2.118	4.39×10^2
z=0.4	22.98	1.375	1.432	2.283	3.900	3.049	2.53
z=1.0	26.82	1.214	1.251	2.469	5.784	4.566	1.80
z=1.5	28.70	0.629	1.107	2.433	6.737	5.410	1.54
z=2.0	29.64	0.486	0.675	1.747	7.263	6.190	1.35
z=3.0	30.86	1.332	0.545	1.139	7.339	6.745	1.08

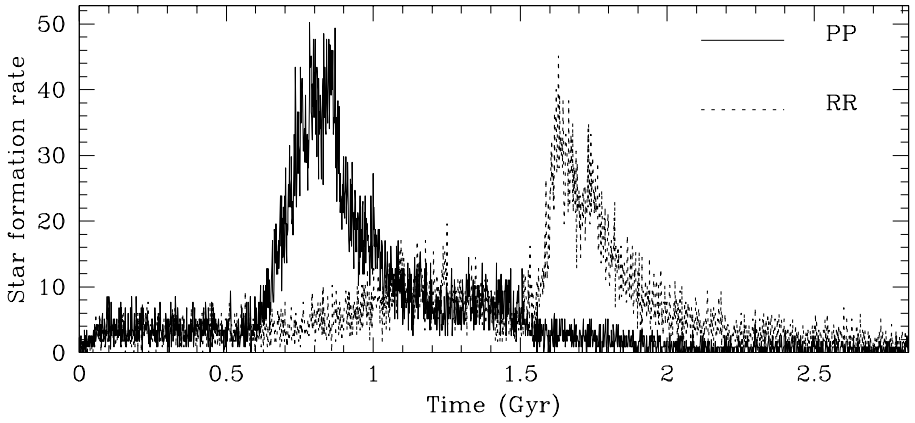

Fig. 1. Star formation history for the PP model (solid line) and the RR one (dotted one). Star formation is given in units of $M_\odot$ yr^{-1} (for the model in which the disk mass and size are 6.0 $\times$ 10^{10} $\mathrm{M}_\odot$ and 17.5 kpc, respectively).

primarily because bulge can greatly suppress the formation of stellar bars during galaxy merging. Accordingly we stress that the derived clear difference in star formation history between the two models (i.e., the PP and RR models) is true only for mergers between two disks without remarkable bulges.

Fig. 2 describes the morphology of a merger at the epoch of its maximum starburst for the PP and RR models. A merger in the present model is the most heavily obscured by dust and shows the strongest far-infrared and sub-millimeter flux at this starburst epoch. As is shown in Fig. 2, young stellar components formed during merging are more compactly distributed in a merger than old stellar ones initially located within disks both for the PP model and for the RR one. This result indicates that compact young stellar components are more heavily obscured by dust than diffuse old ones in a gas-rich major merger. For the PP model, the first and the strongest starburst is triggered at T=0.7 $\sim$ 0.8 Gyr, principally because non-axisymmetric stellar bars formed in the first encounter of the merger excite efficient gas transfer toward the nuclear region of the two disks. Consequently the morphology of the PP merger at T=0.7 Gyr shows two strong and long tidal arms and central bars. As is shown in Fig. 3, dusty interstellar gas is so efficiently transferred to the central region of the stellar bar that the gas can obscure the central starburst component in this PP model. On the other hand, for the RR model, the maximum starburst occurs when two disks finally merge to form an elliptical galaxy (T=1.6 $\sim$ 1.7 Gyr). Strong and long tidal tails are not developed during merging in this RR model, accordingly the morphology at T=1.6 Gyr appears to show no clear signs of tidal interaction. As is shown in Fig. 4, two starburst cores composed mainly of very young stars can be clearly seen in the central 3.5 kpc of the RR merger. The old stellar components, on the other hand, are more diffusely distributed and do not show such distinct two cores in the central region of the RR merger. Dusty inter-

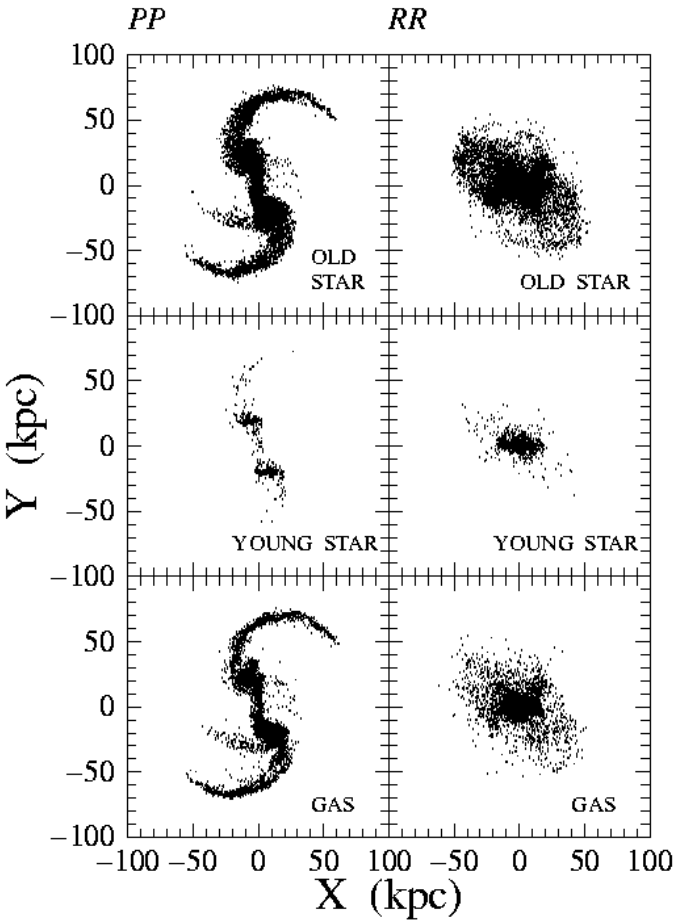

Fig. 2. Mass distribution of a galaxy merger projected onto x-y plane at the epoch of maximum secondary starburst of the merger for the PP model (left) and the RR one (right). Old stars initially located in two disks, young stars formed by secondary starburst, and gas are plotted in the top panel, the middle one, and the bottom one, respectively. Note that strong and long tidal tails can be seen only in the PP model. Note also that young stars are more compactly distributed within a merger than old stars. This result suggests that young stars are more heavily obscured by dusty gas than old stars in a gas-rich merger.

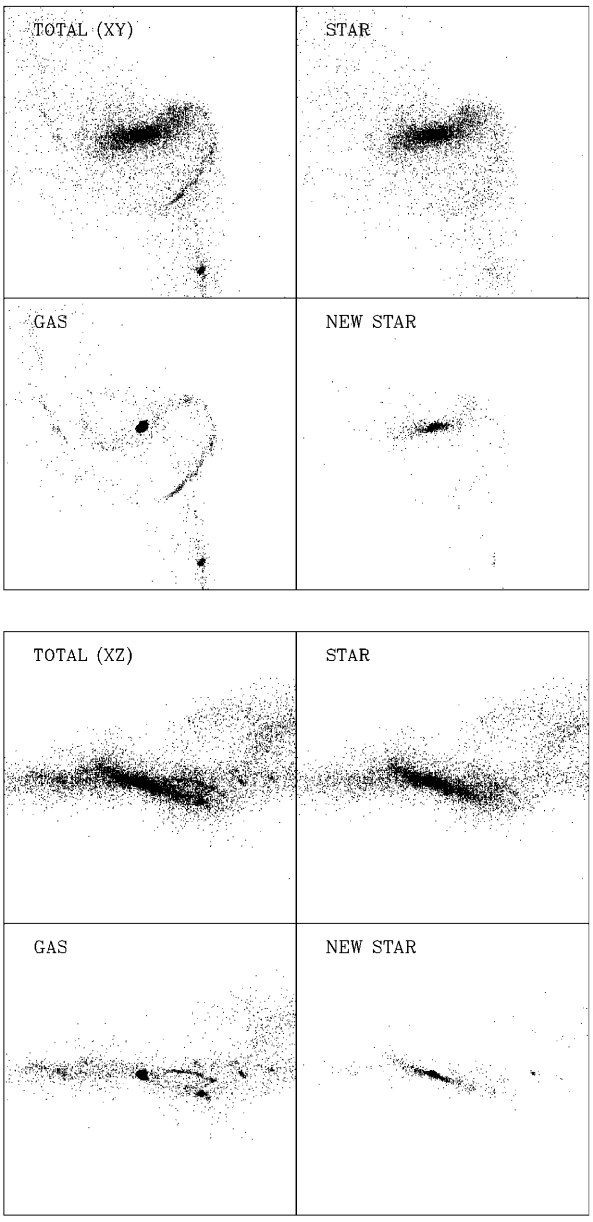

Fig. 3. Mass distribution of the PP model projected onto x-y plane (upper four frames) and x-z one (lower four ones) at T = 0.7 Gyr corresponding to the epoch of maximum starburst of the merger for total components (upper left), old stellar components initially located in two disks (upper right), gaseous ones (lower left), and new stellar ones formed by secondary starburst (lower right). Each of the eight frames measures 35 kpc (2.0 in our units) on a side. Note that the stellar bar is well developed at this massive starburst epoch.

stellar gas is distributed such that it surrounds the two starburst cores. This mass distribution of gas and stars is similar to that found in Arp 220 (e.g., Norris 1985; Sakamoto et al. 1999), which is an ULIRG without long tidal tails (e.g., Sanders & Mirabel 1996; Ohyama et al. 1999). This result for the RR model accordingly suggests that Arp 220 is formed by a nearly retrograde-retrograde merger. These results for the above two models clearly demonstrate that the morphology of a merger at the epoch of its massive dusty starburst depends strongly on the initial orbital configuration.

The derived difference in global morphology between gas-rich major mergers with strong dusty starburst provides important implications for the nature of some ULIRGs, though the present results can be true for mergers without remarkable bulges. Recent high resolution optical/near-infrared imaging of ULIRGs have confirmed that morphology of ULIRGs is very diverse and furthermore that the separation of two galactic cores is very different ranging from 0 kpc (single nuclei) to about $\sim$ 10 kpc (Scoville et al. 2000; Surace et al. 2000). For example, the core separation is estimated to be about 25 kpc for ULIRG IRAS01199-2307 and just 2.5 kpc for IRAS22491-1808 (Surace et al. 2000). Since strong dusty starburst occurs in the first encounter (i.e., when the separation of two disks is an order of 10 kpc) for the PP model without bulges, it is not unreasonable to say that such an ULIRG as IRAS01199-2307 is

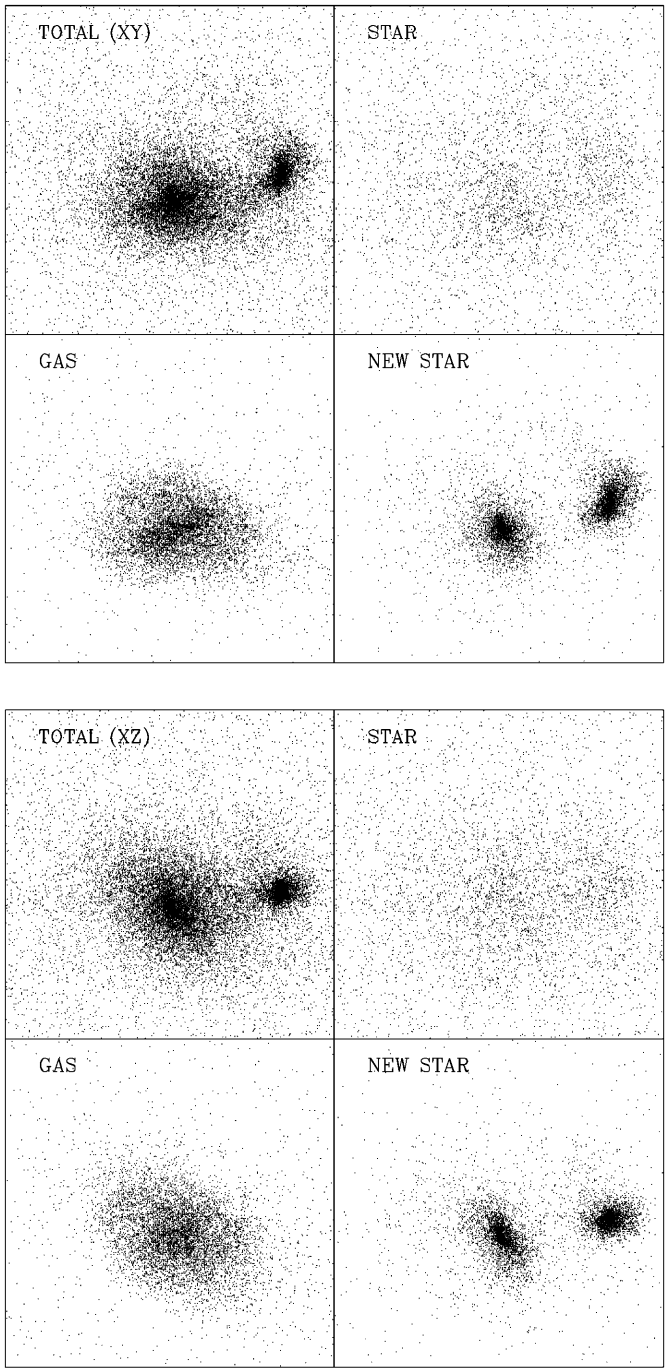

Fig. 4. The same as Fig. 3 but for the RR model at T = 1.6 Gyr. In this figure, each of the eight frames measures 3.5 kpc (0.2 in our units) on a side in order that the central structure can be more clearly seen for this RR model. Note that two distinct cores can be seen only in the new stellar components formed by the star formation in the merger.

formed by a nearly prograde-prograde merger without remarkable bulges. Furthermore, there are several ULIRGs (e.g., IRAS 10173+0828, VIIZw 031) that do not show obvious evidence of current or past interactions (Sanders & Mirabel 1996). Our results suggests that such ULIRGs are formed by mergers that do not produce strong and long tidal tails: ULIRGs without obvious tidal features are formed by nearly retrograde-retrograde mergers. We here do not reject the idea that such ULIRGs are formed by an alternative mechanism (i.e., those other than major merging). The present numerical results imply that the origin of the observed morphological diversity of ULIRGs is due partly to the difference in orbital configurations of major mergers.

Fig. 5 and Fig. 6 show the SED at the epoch of maximum starburst for the two models (PP and RR) with and without dust extinction. By comparing the UV flux with $\lambda < 3000$ Å for the model without dust extinction and that for the model with dust extinction, we can clearly determine to what degree the UV light from secondary starburst is absorbed by dust. Clearly, internal dust extinction of the RR merger is appreciably larger than that of the PP one. The mean value of $A_{\rm V}$ for all stellar components is 1.35 for the PP model and 1.50 for the RR one. Furthermore, if we estimate the mean value of $A_{\rm V}$ in the central 0.5 kpc of a merger at the epoch of maximum starburst, it is 8.06 mag for the upper galaxy and 6.27 mag for the lower one in the PP model and 8.42 mag in the RR one. There are two main reasons for this dependence. The first reason is that owing to a smaller amount of dusty interstellar gas tidally stripped away from the merger, a larger amount of interstellar gas can be transferred to the surroundings of the central compact starburst and thereby obscure the starburst more heavily in the RR model. The second reason is that in the RR model, the massive starburst occurs $only$ one-time and $only$ in the late merger phase when the dusty interstellar gas is the most efficiently transferred to the central region of the merger, and consequently a larger amount of higher density gas can obscure the central starburst. Fig. 2–Fig. 6 therefore imply that both morphology and SED in a dusty starburst merger at the epoch of maximum starburst can be controlled by an initial orbital configuration of the merger and thus that the morphology of the merger can correlate with the SED. To be more specific, a dusty starburst merger without strong and long tidal tails (or with no clear signs of tidal interaction) can show very strong internal dust extinction.

Fig. 7 and Fig. 8 describe how the PP and RR merger models can be observed by the HST if they are located at intermediate and high redshifts ($0.4 \leq z \leq 1$). Table 1 furthermore summarizes the apparent V band magnitude, colours, and submillimeter flux at 850 μm at each redshift for the two models. Most of the observed ULIRGs are located at low redshift (Sanders & Mirabel 1996), these figures are accordingly helpful for deducing morphological properties of intermediate and high redshift ULIRGs. Fig. 7 suggests that the evidence for major merging becomes less clear in optical band at intermediate redshifts for both the PP model and the RR one. This is essentially because the outer low surface brightness tidal feature in a merger is hardly detectable in the present optics of the HST. Compared with the PP model with blue compact morphology ($V-I$ = 2.12 and $m_{\rm I}$ = 20.48 mag), the RR model shows optically faint and very diffuse morphology ($V-I$ = 2.28 and $m_{\rm I}$ = 20.70 mag) owing to the larger dust extinction. We here suggest that some dusty starburst radio sources with optically faint morphology recently discovered by Richards et al. (1999) in deep VLA (Very Large Array) surveys are likely to be these RR

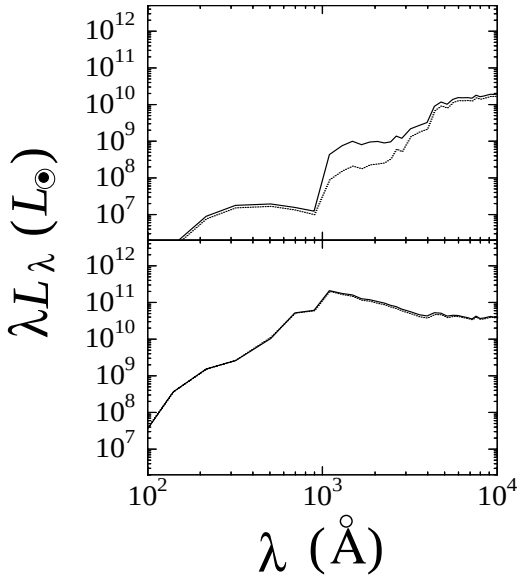

Fig. 5. The upper panel shows the rest-frame SED (with the wavelength less than 10^4 Å) of a galaxy merger at the epoch of its maximum starburst for all stellar components in the PP model (solid line), and for those in the RR one (dotted). For comparison, the SED of a merger without dust extinction and re-emission is also given for each of the two models in the lower panel. Here we can clearly see the effects of dust extinction and re-emission on the SED shape in a merger by comparing the upper panel and the lower one. Note that the difference in UV flux ($\lambda < 3000$ Å) between models with and without dust extinction is larger in the RR model. This indicates that internal dust extinction at the epoch of maximum starburst (i.e., when a merger becomes an ULIRG) is the strongest in the RR model.

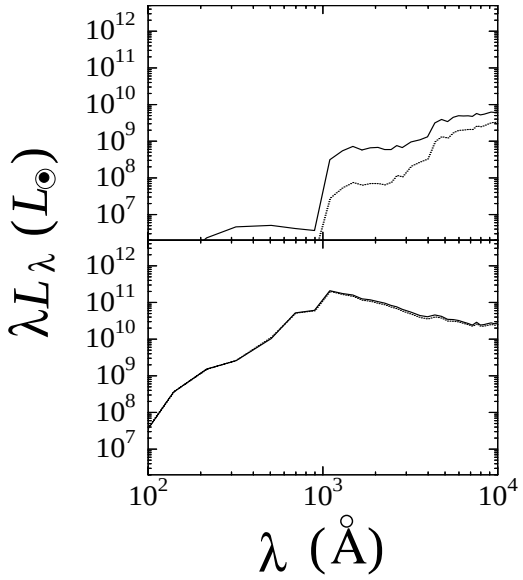

Fig. 6. The same as Fig. 5 but for stellar components within the central 3.5 kpc of the merger in each of the two models.

mergers with the larger dust extinction. As is shown in Fig. 8, near-infrared NIC2 image of the RR merger at z = 0.4 shows more clearly the sign of tidal interaction than WFPC2. However, the RR model with larger extinction shows very faint and diffuse morphology even in the NIC2 at z = 1 and also has redder colours ($R-K \sim 5.8$ mag and $I-K \sim 4.6$ mag). This result implies that $some$ of the observed high-redshift EROs with very faint morphology (e.g., EROs observed by Smail et al. 1999) are formed by major mergers with the larger dust extinction. A growing number of observational results on morphology and spectrophotometric properties of intermediate and high redshift ULIRGs are now being accumulated (e.g. Tran et al. 1998). We accordingly suggest that it is very worthy to observationally confirm whether an intermediate and high redshift ULIRG with no clear signs of tidal interaction preferentially shows the higher degree of internal dust extinction and redder colours and is thus a host galaxy for a faint radio source in VLA surveys and an ERO with optically faint and very diffuse morphology.

4. Discussion

There are several observational results which imply a physical relationship between morphology and photometric properties in ULIRGs. Aurière et al. (1996) found that ULIRGs with no apparent signs of interaction preferentially show the larger ratio of infrared flux to R-band one among ULIRGs with different morphologies and thus suggested that these ULIRGs are highly obscured by internal dust. Arp 220, which is an ongoing merger without strong and long tidal tails and an ULIRGs at z$\sim$0.018 (See Fig. 1 in Ohyama et al. 1999 for the clear morphology of Arp 220), is observed to show very large internal dust extinction with $A_{\rm V} \sim 10$ estimated from optical and near-infrared colours (Scoville et al. 1998) and $A_{\rm V}$ = 45 from near infrared and mid-infrared emission lines (Genzel et al. 1998). The VII Zw031 (IRAS F05081+7936), which also appears to have no strong tidal tails in its R-band image, is found to suffer very strong UV light extinction with the magnitude about 30 times larger than that of other two ULIRGs with clear signs of tidal interaction (Trentham et al. 1999). Two possible interpretations for these ULIRGs with the larger $A_{\rm V}$ are described as follows. One is that these ULIRGs are just in the late merger phase when outer tidal tails become very diffuse and thus less remarkable owing to the dynamical relaxation during merging: Irrespectively of merger orbital configurations, mergers can become ULIRGs with very large $A_{\rm V}$ just in the late merger phase. The other is that the above ULIRGs with very large internal dust extinction can be formed by major mergers that do not produce any strong tidal tails: The above ULIRGs are more likely to be formed by nearly retrograde-retrograde mergers. Considering that $outer$ tidal tail(s) or features can be appreciably seen even in the late phase of galaxy merging (e.g., NGC3921 in Schwizer 1996), the latter interpretation seems to be more plausible. However, since the outer low surface brightness tidal features are hard to be detected especially for distant mergers and ULIRGs (Mihos 1995; Bekki et al. 1999), finer and deeper image data on morphology of ULIRGs are indispensable for determining which interpretation is more plausible for the origin of ULIRGs with very large A_V.

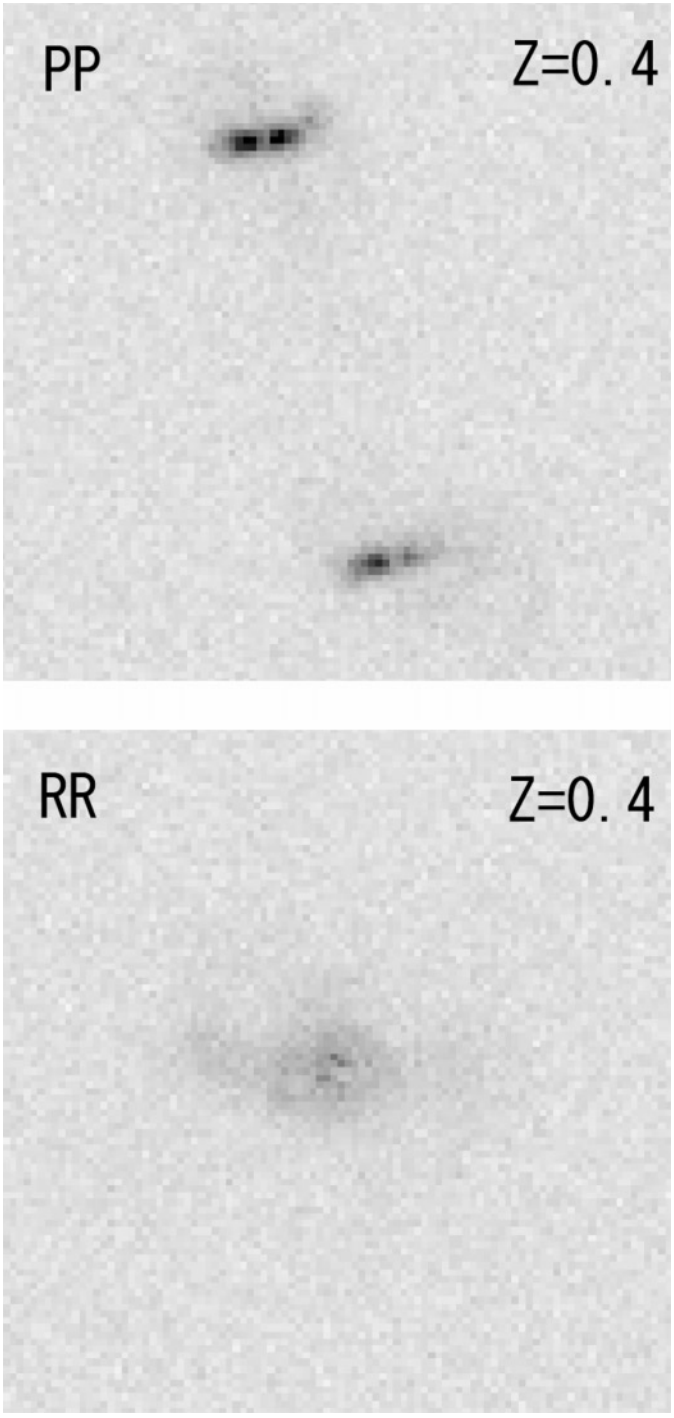

Fig. 7. The HST synthesized image of the PP model (upper panel) and that of the RR one (lower one) at the redshift z=0.4 projected onto the $x-y$ plane corresponding to the orbital plane of the merger for the HST WFPC2 (F814W). In this figure, the morphology of the merger at the epoch of the maximum starburst ($T = 0.7$ Gyr for the PP model and T = 1.6 Gyr for the RR one) is described. The method to create this synthesized image is described in detail by Bekki et al. (1999). The exposure time for each synthesized morphology is set to be 10^4 sec (2000 sec $\times 5$) for the HST WFPC2. Each frame measures $9.''9$ corresponding to 63.7 kpc on a side and one pixel size is $0.''1$ for the WFPC2.

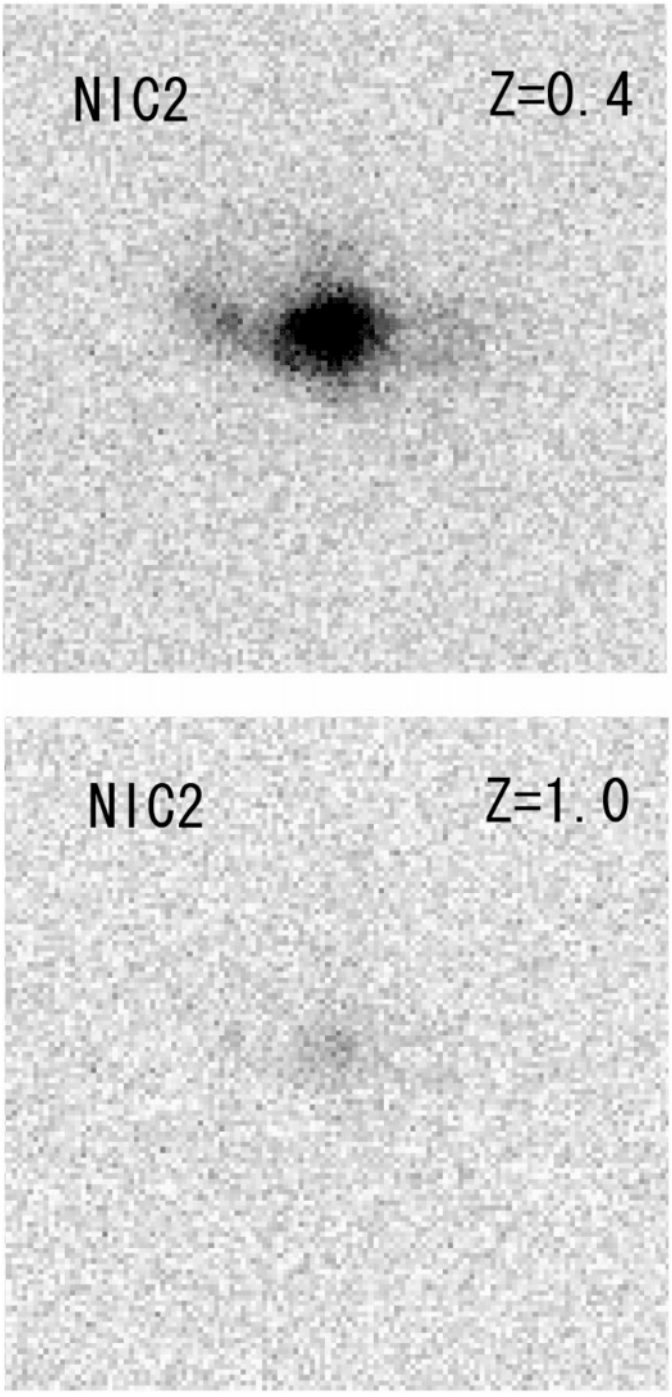

Fig. 8. The HST synthesized image of the RR model at the redshift z=0.4 (upper) and 1.0 (lower) for the HST NIC2 (F160W). In this figure, the morphology of the merger at the epoch of the maximum starburst ($T = 1.6$ Gyr) is described. The exposure time for each synthesized morphology is the same as that of the WFPC2 (10^4 sec) in Fig. 3. Each frame measures $9.''9$ (corresponding to 63.7 kpc) on a side and one pixel size is $0.''076$ for the NIC2.

The present results furthermore provide an important clue to the physical origin for the observed colour differences between high redshift (z $\geq$ 1.0) faint SCUBA sources. Smail et al. (1998, 1999) revealed that $V-I$ colour is very different between faint SCUBA sources and discovered two EROs with $I-K \geq 6.0$ and 6.8 among SCUBA sources. The origin for this observed colour differences, which can result from several factors such as differences in internal dust extinction, redshifts, and the energy flux ratio of thermal starburst activity to non-thermal AGN between SCUBA sources, has not been clarified at all. As is described in the Table 1, our dusty starburst models with 850μm flux ranging from 1.4 to 2.2 mJy for $1 \leq z \leq 2$ predict that the $R-K$ ($I-K$) colours at z=1, 1.5, and 2 are 5.38 (4.29), 5.96 (4.99), and 6.07 (5.43), respectively, for the PP model and 5.78 (4.57), 6.74 (5.41), and 7.26 (6.19), respectively, for the RR one. These results therefore imply that one of important factors for the observed colour differences between faint SCUBA sources is the difference in orbital configurations between higher redshift major galaxy mergers with dusty starburst. One of observational tests which can assess the validity of this interpretation is to reveal the physical relationship between the detailed morphology of SCUBA sources and their colours (or SEDs). It is, however, considerably difficult even for the present optics of the HST to reveal the detailed morphology of high redshift mergers (Mihos 1995; Bekki et al. 1999). Thus future large space and ground-based telescopes will discover the fine structure of high redshift SCUBA sources and EROs and thereby clarify the relative importance of merger orbital configurations in determining the SEDs and colours in high-redshift dusty starburst galaxies.

Acknowledgements. Y.S. thanks to the Japan Society for Promotion of Science (JSPS) Research Fellowships for Young Scientist.

References

Aurière M., Hecquet J., Coupinot G., Arthaud R., Mirabel I.F., 1996, A&A 312, 387
Barger A.J., Cowie L.L., Sanders D.B., et al., 1998, Nat 394, 248
Barnes J., Hernquist L., 1992, ARA&A 30, 705
Bekki K., Shioya Y., 1999, ApJ 513, 108
Bekki K., Shioya Y., 2000, ApJ in press
Bekki K., Shioya Y., Tanaka I., 1999, ApJ 520, L99
Bruzual A.G., Charlot S., 1993, ApJ 405, 538
Elston R., Rieke G.H., Rieke M.J., 1988, ApJ 331, L77
Fall S.M., Efstathiou G., 1980, MNRAS 193, 189
Franceschini A., Mazzei P., De Zotti G., Danese L., 1994, ApJ 427, 140
Genzel R., et al., 1998, ApJ 498, 579
Gordon K., Calzetti D., Witt A.N., 1997, ApJ 487, 625
Guiderdoni B., Hivon E., Bouchet F.R., Maffei B., 1998, MNRAS 295, 877
Holland W.S., Robson E.I., Gear W.K., et al., 1999, MNRAS 303, 659
Hughes D. Serjeant, S., Dunlop J., et al., 1998, Nat 394, 241
Lilly S.J., Eales S.A., Gear W.K.P., et al., 1999, ApJ 641, 518
Mazzei P., Xu C., De Zotti G., 1992, A&A 256, 45
Meurer G.R., Heckman T.M., Calzetti D., 1999, ApJ 521, 64
Mihos J.C., 1995, ApJ 438, L75
Mihos J.C., Hernquist L., 1996, ApJ 464, 641
Norris R.P., 1985, MNRAS 216, 701
Ohyama Y., Taniguchi Y., Hibbard J.E., Vacca W.D., 1999, AJ 117, 2617
Richards E.A., Formalont E.B., Kellermann K.I., et al., 1999, ApJ 526, L73
Sakamoto K., Scoville N.Z., Yun M. S., et al., 1999, ApJ 514, 68
Sanders D.B., Soifer B.T., Elias J.H., et al., 1988a, ApJ 325, 74
Sanders D.B., Mirabel I.F., 1996, ARA&A 34, 749
Schmidt M., 1959, ApJ 344, 685
Schwarz M.P., 1981, ApJ 247, 77
Schwizer F., 1996, AJ 111, 109
Scoville N.Z., Evans A.S., Dinshaw N., et al., 1998, ApJ 492, L107
Scoville N.Z., Evans A.S., Thompson R., et al., 2000, AJ 119, 991
Smail I., Ivison R.J., Blain A.W., 1997, ApJ 490, L5
Smail I., Ivison R.J., Blain A.W., Kneib J.-P., 1998, ApJ 507, L21
Smail I., Ivison R.J., Kneib J.-P., et al., 1999, MNRAS 308, 1061
Surace J.A., Sanders Evans A.S., 2000, ApJ 529, 170
Tran H.D., Brotherton M.S., Stanford S.A., van Breugel W., 1998, preprint (astro-ph/9811322)
Trentham N., Kormendy J., Sanders D.B., 1999, AJ 117, 2152
Zaritsky D., Kennicutt R.C., Huchra J.P., 1994, ApJ 420, 87